

Transformers Remember First, Forget Last: Dual-Process Interference in LLMs

Sourav Chattaraj
Thomson Reuters

sourav.chattaraj@thomsonreuters.com

Kanak Raj
Thomson Reuters

kanak.raj@thomsonreuters.com

Abstract

When large language models encounter conflicting information in context, which memories survive—early or recent? We adapt classical interference paradigms from cognitive psychology to answer this question, testing 39 LLMs across diverse architectures and scales. Every model shows the same pattern: proactive interference (PI) dominates retroactive interference (RI) universally (Cohen’s $d = 1.73$, $p < 0.0001$), meaning early encodings are protected at the cost of recent information—the opposite of human memory, where RI typically dominates.

Three findings indicate that RI and PI reflect separate memory mechanisms. RI and PI are uncorrelated ($R^2 = 0.044$), rejecting a unified “memory capacity.” Model size predicts RI resistance ($R^2 = 0.49$) but not PI ($R^2 = 0.06$, n.s.)—only RI is capacity-dependent. And error analysis reveals distinct failure modes: RI failures are passive retrieval failures (51%), while PI failures show active primacy intrusion (56%); both show $<1\%$ hallucination. These patterns parallel the consolidation–retrieval distinction in cognitive science, suggesting that transformer attention creates a primacy bias with direct implications for interference-heavy applications.

1 Introduction

When humans learn new information that conflicts with prior knowledge, the new typically disrupts recall of the old—*retroactive interference* (RI). The reverse, where prior knowledge blocks new learning, is *proactive interference* (PI). A century of research establishes that human memory shows $RI > PI$: recent information overwrites earlier memories more readily than earlier memories block recent ones (Jenkins and Dallenbach, 1924; Underwood, 1957).

Consider a medical AI tracking a patient’s blood pressure across a 12-hour emergency visit: 120

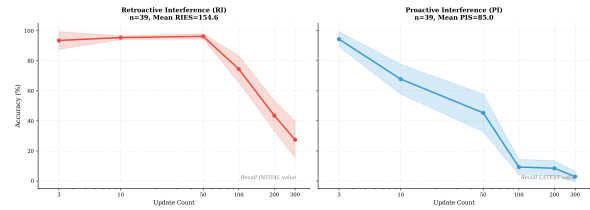


Figure 1: **LLMs Show Opposite Interference Pattern to Humans.** Retroactive interference (RI, left) maintains near-ceiling accuracy through $N=50$ (96%), then drops sharply to 27% at $N=300$. Proactive interference (PI, right) collapses accuracy from 85% to 2%—near-complete failure. All 39 models show $PI > RI$, contrasting with human memory where RI dominates. Shaded regions: 95% CI.

mmHg at triage, 135 after 15 minutes, 128 post-medication, 118 at discharge. When the physician asks “What was the initial blood pressure?” (RI task), the system must recall the first value despite three subsequent updates. When asked “What is the current blood pressure?” (PI task), it must access the most recent value despite earlier readings competing for attention. These scenarios demand opposite memory operations—and our findings suggest LLMs handle them very differently.

Despite remarkable advances in few-shot learning and reasoning (Brown et al., 2020; Achiam et al., 2023), and context windows expanding to millions of tokens, how LLMs handle memory interference remains poorly understood. We adapted classical interference paradigms from cognitive psychology to test 39 large language models. **Every single model shows the opposite pattern:** PI dominates RI across all architectures, scales, and training regimes (Cohen’s $d = 1.73$, $p < 0.0001$). Transformers protect early encodings at the cost of recent information—the inverse of biological memory (Figure 1).

This inversion is not merely surprising—it suggests distinct computational structure. If RI and PI reflected unified “memory capacity,” they would

correlate strongly. Instead, they are essentially independent ($R^2 = 0.044$). Model size correlates with RI resistance but not PI resistance. Error analysis reveals distinct failure modes: RI failures are passive (models cannot retrieve), while PI failures are active (earlier values intrude). Both show minimal hallucination—models confuse positions rather than fabricate.

These dissociations suggest RI and PI engage computationally distinct mechanisms, paralleling the consolidation–retrieval distinction in cognitive science (Wixted, 2004). RI appears to test whether initial encodings can resist overwriting—a capacity-limited process scaling with parameters. PI tests whether attention can favor recent over competing earlier information—an architectural constraint independent of scale.

Prior LLM memory research has focused on PI (Wang and Sun, 2025), leaving RI unexplored. Yet applications from medical records to legal documents require recalling initial states after updates. Understanding how these interference types differ is essential for principled deployment.

Contributions.

1. **Evidence consistent with dual-process memory:** RI and PI are uncorrelated ($R^2 = 0.044$) with opposite scaling relationships, suggesting consolidation-based RI (capacity-dependent) versus retrieval-based PI (capacity-independent).
2. **Inverted interference profile:** All tested LLMs show $PI > RI$ ($d = 1.73$), contrasting with human memory where RI typically dominates—suggesting transformer attention produces primacy protection absent in biological systems.
3. **Cognitive failure taxonomy:** RI failures are passive (retrieval failure), PI failures are active (primacy intrusion), both with minimal hallucination—position confusion, not fabrication.

2 Background

Interference in Human Memory. Retroactive interference (RI) and proactive interference (PI) have been studied since the 1920s as fundamental constraints on human memory (Jenkins and Dallenbach, 1924; Underwood, 1957). RI occurs when new learning disrupts recall of prior material; PI occurs when prior learning blocks recall of new

material. In serial recall, humans typically show both primacy and recency effects, with recency dominating immediate recall (Murdock, 1962)—a pattern our LLM results will contrast with. Importantly, the relative magnitude of RI versus PI is *not universal*—it depends on experimental conditions including semantic similarity, retention interval, degree of original learning, and individual differences (MacLeod, 2024). While RI often dominates in immediate paired-associate learning (the paradigm closest to our experiments), some conditions favor PI dominance, particularly with extended prior learning or category shifts (Wickens, 1970). Working memory capacity predicts interference resistance (Engle, 2002; Kane and Engle, 2001). Modern theories, building on dual-store models of memory (Atkinson and Shiffrin, 1968), distinguish two mechanisms (Wixted, 2004): *consolidation-based* interference (RI), where new learning overwrites insufficiently stabilized memories, and *retrieval-based* interference (PI), where competing traces disrupt cue-driven recall, with stronger memories actively suppressing weaker competitors (Anderson et al., 1994). This consolidation–retrieval distinction provides our framework for interpreting LLM interference patterns.

Memory Interference in LLMs. We distinguish *in-context interference*—competition between items within a single forward pass—from *catastrophic forgetting*, where new training overwrites prior knowledge in model weights (McCloskey and Cohen, 1989; French, 1999). Our work addresses the former: can models maintain access to information when semantically similar content creates competition? Existing long-context benchmarks primarily test search—whether models can locate specific information within extended contexts (Kamradt, 2023; Bai et al., 2024; Modarressi et al., 2025; Fu et al., 2025; Ling et al., 2025). These tasks confound retrieval difficulty with context length, leaving open whether models can maintain information under semantic conflict. Transformer attention also exhibits known positional biases—models struggle with middle positions (Liu et al., 2024) and disproportionately attend to initial tokens (Xiao et al., 2024)—but how these biases interact with memory interference remains untested. Wang and Sun (2025) conducted the first systematic study of PI in LLMs, finding that model size predicts resistance ($R^2 = 0.26$) while context length does not. However, retroactive interference—

whether LLMs can recall initial information after conflicting updates—remains unexplored. More broadly, while scaling laws predict general capability improvements with size (Kaplan et al., 2020; Hoffmann et al., 2022), whether RI and PI scale differently has not been tested. This gap matters both theoretically and practically: if RI and PI tap distinct mechanisms (consolidation vs. retrieval), models may show different vulnerability profiles; if they reflect unified capacity, performance should correlate. We address this by adapting classical AB-AC interference paradigms (Underwood, 1957) to test both RI and PI on identical stimulus sequences, enabling direct comparison across 39 LLMs.

3 Methods

Task Design. We adapt the classic AB-AC interference paradigm from cognitive psychology (Underwood, 1957) to probe LLM memory. Models first learn 46 category-value pairs (e.g., `visual art: impressionism`), then process N interleaved updates per category ($N \in \{3, 10, 50, 100, 200, 300\}$), where each update assigns a new value to a previously seen category (e.g., `visual art: baroque`). We then query either the initial value (retroactive interference, RI) or the most recent value (proactive interference, PI). Critically, RI and PI use identical stimulus sequences—only the query target differs—enabling controlled comparison (Figure 2).

Dataset. We constructed a dataset of 46 semantic categories with real-world meaningful values per category. Updates are randomly interleaved across categories without grouping updates for the same key contiguously—mimicking concurrent updates in real-world data logs. This setup ensures interference arises from semantic competition, not positional proximity. Details in Appendix A.

Metrics. To capture overall interference resistance (not just performance at one level), we compute the **Retroactive Interference Endurance Score (RIES)**—the area under the accuracy-vs-interference curve, log-scaled to weight performance equally across interference magnitudes:

$$\text{RIES} = \int_{N=3}^{300} A_{\text{RI}}(N) d(\log_{10}(N+1)) \quad (1)$$

where $A_{\text{RI}}(N)$ is retrieval accuracy for initial values at interference level N . A model scoring 100% accuracy at all levels achieves $\text{RIES} \approx 200$; a model

at 50% throughout scores ≈ 100 . **PIES** (Proactive Interference Endurance Score) uses the identical formula applied to accuracy for most-recent values. Higher scores indicate stronger resistance to interference. Thus, $\text{RIES} > \text{PIES}$ means a model resists RI better than PI—equivalently, PI causes more performance degradation than RI.

Models. We tested 39 LLMs with complete data across all interference levels, spanning 1B–2.5T parameters. Models include open-weight (Llama, Mistral, Qwen) and proprietary (GPT-4o, Claude-3.5, o1, o3) architectures, with context windows from 8K to 2M tokens. Both RI and PI experiments used 3 independent runs per model; results showed high consistency (RI: 73.7% zero variance, 90.2% $\text{SD} < 5$; PI: 64.8% zero variance, 90.4% $\text{SD} < 5$; see Figure 10 for distribution). Full specifications in Appendix B.

4 Results

4.1 Retroactive Interference in LLMs

All 39 tested models exhibit substantial retroactive interference. At minimal interference ($N = 3$ updates per category), mean accuracy is 93.5% ($\text{SD}=4.96\%$). Accuracy remains high through $N = 50$ (96.3%, reflecting ceiling effects), then drops sharply: 74.5% at $N = 100$, 43.5% at $N = 200$, and 27.4% at $N = 300$. This 66-point drop from peak confirms that LLMs struggle to recall initial information when subsequent updates create semantic conflict—establishing RI as a robust phenomenon warranting mechanistic investigation.

Performance varies substantially across models (Table 1). Top performers (o1, Claude-3.5-sonnet) maintain above 60% accuracy even at maximum interference, while bottom performers (smaller Llama variants) drop below 10%. This $6\times$ range motivates our investigation of what factors predict resistance.

4.2 Model Size Correlates with RI Resistance

What determines whether a model resists retroactive interference? We tested two candidate predictors: model size (parameter count) and context window length.

Size correlates with RI resistance. Linear regression reveals that parameter count accounts for 49% of variance in RIES—our aggregate measure of accuracy maintained across all interference levels ($R^2 = 0.491$, $\beta = 0.70$, $p < 0.0001$; Figure 3).

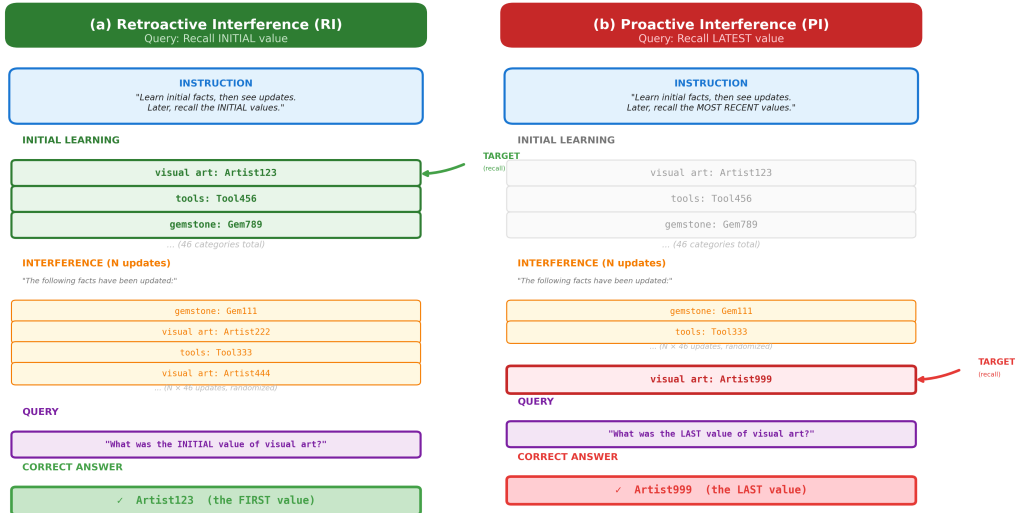


Figure 2: **Experimental Paradigm.** Both RI and PI use identical sequences: 46 initial facts followed by N updates. RI queries initial values (green); PI queries final values (red). This isolates interference from search difficulty.

Table 1: **RI Resistance Varies Widely.** Top 5 and bottom 5 models by RIES, showing accuracy at low ($N=3$) and high ($N=300$) interference.

Model	RIES	Acc@3	Acc@300
<i>Top 5</i>			
o1	186.4	100%	86%
o3	185.8	100%	83%
o3-mini	183.3	100%	79%
Claude-3.5-sonnet	178.2	98%	62%
GPT-4o	176.1	97%	58%
<i>Bottom 5</i>			
Llama-3.2-3b	113.2	82%	4%
Mistral-7b	121.5	85%	8%
Qwen-2.5-7b	128.7	88%	12%
Gemma-2-9b	131.4	89%	15%
Llama-3.1-8b	134.6	90%	18%

Models in the largest size tier ($>500\text{B}$ parameters) achieve mean RIES of 171.2, compared to 142.8 for the smallest tier ($<10\text{B}$)—a 28-point advantage, with ANOVA confirming a significant monotonic size effect ($F(3, 35) = 11.83, p < 0.0001$).

Context length does not. Context window size shows no relationship with RIES ($R^2 = 0.003, p = 0.746$). A model with 32K context and 100B parameters outperforms a model with 1M context and 10B parameters. This dissociation suggests that interference resistance reflects representational capacity, not buffer size.

Critically, size does NOT predict PI resistance. When we apply the same regression to PIES (the

equivalent metric for PI), model size explains only 6% of variance ($R^2 = 0.06, p = 0.14, \text{n.s.}$). This asymmetry—size predicting RI but not PI—provides first evidence that the two interference types engage different mechanisms.

Mechanistic interpretation. We attribute this asymmetry to *superposition* (Elhage et al., 2022): smaller models represent features with overlapping vectors, creating interference; larger models allocate more orthogonal representations. For RI, this representational room lets initial encodings survive alongside updates. For PI, the bottleneck is attention selection, not representation—an architectural constraint unaffected by capacity (see Discussion).

4.3 Reasoning Models Excel at RI—With a Hidden Cost

Do architectural innovations beyond scale affect interference resistance? We compared chain-of-thought reasoning models (Wei et al., 2022; OpenAI, 2024) (o1, o3, o4-mini, DeepSeek-R1; $n=6$) against standard models ($n=33$).

Reasoning models show 18% higher RIES. Mean RIES for reasoning models is 178.0 (SD=12.6) versus 150.3 (SD=18.2) for non-reasoning models—an 18.4% advantage (independent $t(37) = 3.54, p = 0.001$, Cohen’s $d = 1.76$). Five of six reasoning models rank in the top 10 for RI resistance. Extended inference-time computation appears to enhance memory consolidation.

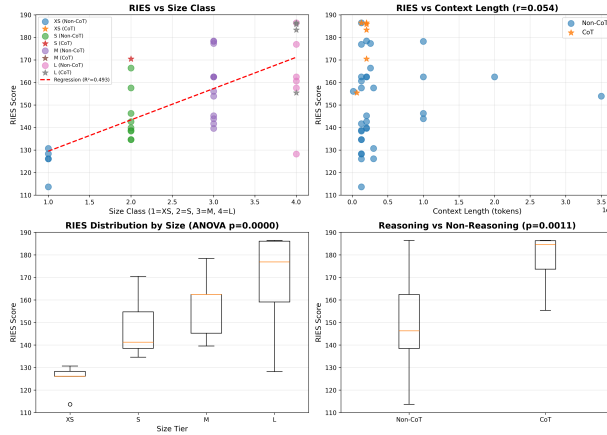


Figure 3: **Size Predicts RI Resistance, Not PI.** (A) Model size vs RIES shows strong positive relationship ($R^2 = 0.49$, $p < 0.0001$). (B) Context length vs RIES shows no relationship ($R^2 = 0.003$, n.s.). Size-PI relationship: $R^2 = 0.06$, n.s.—size does not predict PI resistance (see Figure 6 in Appendix).

But this advantage does not transfer to PI.

The same reasoning models that excel at RI show no advantage—and often disadvantage—for PI. Most strikingly, o1 ranks #1 for RI (RIES = 186.4) but #35 for PI (PIES = 21.9), an $8.5\times$ asymmetry. This dissociation further demonstrates that RI and PI tap different mechanisms: reasoning aids consolidation but does not help—and may hurt—recency access.

Practical implication: Reasoning models are optimal for applications requiring robust historical memory (document analysis, knowledge retrieval), but suboptimal for tasks requiring recent-state tracking (dialogue, real-time updates).

4.4 Decay Patterns Reveal Architectural Diversity

How does accuracy degrade as interference increases? Unlike PI, which follows a universal log-linear decline across all models (Wang and Sun, 2025), RI decay shows striking architectural diversity. Fitting decay functions to each model’s accuracy curve reveals: 35% follow exponential decay (rapid early forgetting), 30% polynomial (gradual degradation), 26% log-quadratic (initial resistance then collapse), and 9% power-law (O-series reasoning models). This heterogeneity suggests different architectures implement memory consolidation differently, while retrieval competition (PI) operates through shared attention mechanisms. The architectural fingerprint in decay patterns provides further evidence that RI and PI engage distinct computational processes.

4.5 RI and PI Engage Distinct Mechanisms

If RI and PI reflect a unified “memory capacity,” models good at one should be good at the other. We tested this by correlating RIES and PIES across all 39 models.

RI and PI are uncorrelated. Pearson correlation yields $r = 0.21$ ($R^2 = 0.044$, $p = 0.201$; Figure 4). Knowing a model’s RI performance tells you essentially nothing about its PI performance. This rejects the unified-capacity hypothesis and suggests RI and PI tap computationally distinct processes.

All models show PI > RI. Despite this independence, a striking asymmetry emerges: every tested model (39/39, 100%) shows higher RIES than PIES. The mean difference is 69.5 points (paired $t(38) = 10.71$, $p < 0.0001$, Cohen’s $d = 1.73$). This is a large effect—LLMs find proactive interference substantially harder than retroactive interference.

This contrasts with typical human findings. In human memory, retroactive interference typically dominates (Underwood, 1957): new information disrupts old more than old disrupts new. LLMs show the opposite. Transformer attention mechanisms appear to create “primacy protection”—early encodings are preserved at the cost of recency access.

4.6 Asymmetry Magnitude Varies by Architecture

While all models show PI > RI, the *magnitude* of asymmetry varies dramatically across model families, revealing distinct architectural trade-offs in memory system design:

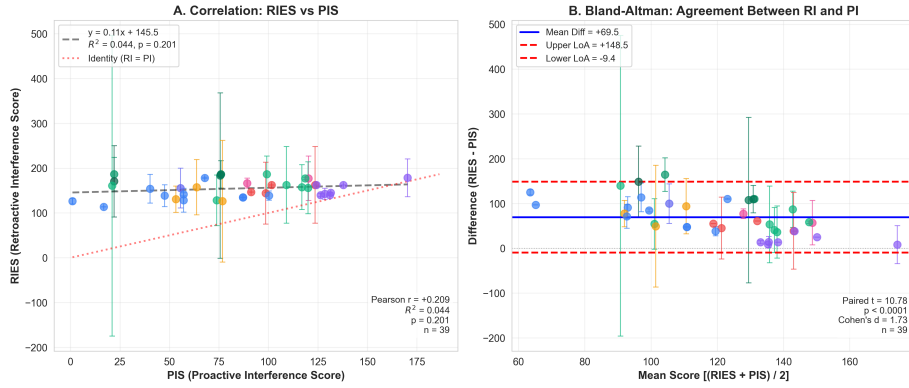


Figure 4: **RI and PI: Uncorrelated with Systematic Bias.** (A) Scatter plot shows weak correlation ($R^2 = 0.044$, $p = 0.20$); all points above diagonal indicate universal RIES > PIES. (B) Bland-Altman plot reveals systematic bias of +69.5 points (95% limits: -9.4 to $+148.5$), confirming RI and PI are not interchangeable measures.

- **O-Series (Extreme):** o1 ranks #1 for RI (RIES = 186.4) but #35 for PI (PIES = 21.9)—an $8.5\times$ asymmetry. Chain-of-thought reasoning optimizes consolidation at the cost of recency.
- **Claude (Minimal):** Claude-4.5-opus shows RIES = 178.4 and PIES = 170.3—only $1.05\times$ asymmetry. Seven of the top 10 PI performers are Claude models, suggesting balanced memory design.
- **GPT (Moderate):** GPT-5 shows $1.9\times$ asymmetry, occupying the middle ground between extremes.

This 8-fold range in asymmetry magnitude demonstrates that the universal $PI > RI$ pattern admits substantial architectural variation. Reasoning architectures appear to sacrifice recency for historical accuracy; Claude’s balanced design suggests deliberate optimization for both. These patterns provide principled guidance for model selection: applications requiring robust historical memory should prefer O-series, while those requiring recent-state tracking should prefer Claude.

4.7 Error Analysis Reveals Distinct Failure Modes

To understand *why* RI and PI engage different mechanisms, we analyzed 5,409 RI errors and 9,753 PI errors across all models. We classified errors into five categories: (1) retrieval failure—no value returned; (2) same-key interference—value from correct category, wrong position; (3) cross-key interference—value from different category; (4) hallucination—value never presented; (5) partial match—close but not exact match.

RI and PI show distinct error signatures (Ta-

ble 2). RI failures are predominantly retrieval failures (50.8%)—models cannot access any value for the queried category. PI failures are predominantly same-key intrusions (56.1%)—models return earlier values from the correct category, suggesting active competition from prior encodings.

Minimal hallucination in both. Critically, hallucination rates are below 1% for both RI (0.8%) and PI (0.6%). Models do not fabricate values—they confuse positions within seen information. This suggests interference is a retrieval/selection problem, not a generation problem.

Metacognitive awareness is PI-specific. Not all retrieval failures are silent. Using LLM-as-judge classification, we find that 8.6% of PI retrieval failures involve explicit refusals (“I’m sorry, but I can’t determine that from the provided text”), compared to 0% for RI. This asymmetry is striking: models recognize when old memories compete with recent information, but fail to detect when recent information overwrites earlier ones. In transformer terms, PI creates multiple attention candidates for the same query—the model can “sense” competing activations and refuse. RI simply dilutes attention to the target position; with no competing signal, the model confidently returns whatever value receives strongest (but incorrect) attention.

Interpretation. RI failures appear “passive”: the initial encoding was overwritten or inaccessible, leaving nothing to retrieve. PI failures appear “active”: earlier encodings intrude on attempts to access recent information. This passive/active distinction aligns with the consolidation (RI) vs. retrieval competition (PI) framework from cognitive science.

Position bias confirms the mechanism. When

Table 2: **Error Distribution: RI vs PI.**

Error Type	RI (%)	PI (%)
Retrieval failure	50.8	42.5
Same-key intrusion	46.0	56.1
Cross-key intrusion	0.6	0.7
Hallucination	0.9	0.2
Partial match	1.8	0.7

same-key intrusions occur, *where* do the incorrect values come from? RI intrusions show recency bias: errors come from middle-to-late positions (mean normalized position = 0.51, where 0 = first update, 1 = most recent). The interfering content “wins”—models return recent values when asked for initial ones. PI intrusions show primacy bias: errors come from early positions, with 14% of errors returning the *first* value presented. The initial encoding persists and blocks access to updates. This contrast is sharpest at minimal interference ($N = 3$): RI errors come from position 0.72 (late) versus PI errors from 0.12 (early). This opposing directionality—RI errors from late, PI errors from early—provides direct mechanistic evidence that the two interference types engage opposite retrieval dynamics.

5 Discussion

Evidence Consistent with Dual-Process Memory.

The central finding of this work is that retroactive and proactive interference appear to engage computationally distinct mechanisms in LLMs. Three lines of evidence support this claim. First, RIES and PIES are uncorrelated ($R^2 = 0.044$)—knowing a model’s RI performance tells you almost nothing about its PI performance. Second, model size correlates with RI resistance ($R^2 = 0.49$) but not PI resistance ($R^2 = 0.06$, n.s.)—only RI appears capacity-dependent. Third, error profiles differ qualitatively: RI failures are passive (retrieval failure dominates), while PI failures show active intrusion from earlier positions—mirroring retrieval-induced forgetting (Anderson et al., 1994), where stronger memory traces actively suppress weaker competitors from the same category.

This pattern parallels the consolidation–retrieval distinction in cognitive science (Wixted, 2004). RI appears to test whether initial encodings can resist overwriting—a process requiring representational capacity that scales with parameters. PI tests whether attention mechanisms can favor recent over competing earlier information—an architectural

constraint independent of scale.

Superposition May Explain the Capacity Dependence.

Why does size predict RI but not PI? The superposition hypothesis (Elhage et al., 2022) provides a mechanistic answer. When neural networks must represent more features than they have dimensions, they encode features as nearly-orthogonal vectors that partially overlap—creating interference between similar representations. Smaller models, with fewer parameters, are forced into greater superposition; larger models can allocate more orthogonal representations (Scherlis et al., 2022). For RI, where the initial category-value pair must survive alongside subsequent updates, representational overlap causes the initial encoding to be “blurred” by later ones. Larger models reduce this overlap, preserving the initial encoding. For PI, the challenge is fundamentally different: all values may be distinctly represented, but attention must *select* the correct one. Attention’s primacy bias—reinforcing early tokens throughout the forward pass—is an architectural property that additional parameters cannot override. This is consistent with RI being capacity-limited (benefiting from reduced superposition) while PI is architecture-constrained (limited by attention dynamics).

Why Transformers Differ from Humans.

Human memory consistently shows $RI > PI$ (Underwood, 1957)—new information disrupts old more than old disrupts new. LLMs show the universal opposite: all 39 models exhibit $PI > RI$. Where human serial position curves show recency dominance in immediate recall (Murdock, 1962), LLMs exhibit primacy dominance—inverting the canonical pattern. We attribute this to self-attention’s inherent bias toward early positions, consistent with the positional biases introduced earlier: the “lost in the middle” effect, where models struggle with information in middle positions (Liu et al., 2024), and “attention sinks,” where initial tokens receive disproportionate attention regardless of content (Xiao et al., 2024). In causal attention, early tokens accumulate attention from all subsequent positions, while later tokens can only attend backward. This creates asymmetric representational strength: early encodings are reinforced throughout the forward pass; recent tokens lack this cumulative advantage. The result is “primacy protection”—a feature, not a bug, of the architecture—that preserves distant context at the cost of recency.

Table 3: **Empirical Observations from Our Paradigm.** Key findings; generalization to specific applications requires validation.

Model Characteristic	Observed Pattern
Reasoning models	18% higher RI resistance; lowest PI resistance
Large dense models	Strong RI and PI; balanced performance
Parameter count	Predicts RI ($R^2=0.49$), not PI ($R^2=0.06$)
Context length	No predictive value for either RI or PI

Practical Implications. Our findings suggest one empirically-supported principle: **parameter count matters more than context length** for interference resistance—a 100B model with 32K context outperformed a 10B model with 1M context in our paradigm. Table 3 summarizes key empirical observations; however, we emphasize that (1) these derive from a single experimental paradigm, (2) the exact nature of each application determines which interference type matters more, and (3) many factors beyond RI/PI characteristics affect model selection. Application-specific validation is essential before deployment.

6 Conclusion

We presented the first systematic comparison of retroactive and proactive interference in LLMs, providing evidence that these phenomena may engage distinct computational mechanisms rather than reflecting unified memory capacity. Three findings inform understanding of transformer memory: (1) RI and PI are uncorrelated ($R^2 = 0.044$) with opposite scaling relationships—RI appears capacity-dependent, PI does not; (2) all 39 tested models show $PI > RI$ ($d = 1.73$), contrasting with the typical human pattern where RI dominates; (3) error analysis supports the distinction—RI failures are passive (retrieval failure), PI failures are active (primacy intrusion), both with minimal hallucination.

These results suggest that transformers exhibit fundamentally different interference profiles from biological memory: attention mechanisms appear to protect early encodings at the cost of recency.

Future Directions. Three directions extend this work. First, *ecologically valid benchmarks*: our synthetic category-value paradigm should be complemented by long-running narratives where facts evolve organically (Kočísky et al., 2018) and semi-

structured evolving documents—medical case logs, legal case files, news timelines—where factual updates are critical and ground truth remains verifiable. Second, *mechanistic validation*: attention probing on open-weight models can directly test whether early tokens accumulate disproportionate attention, and analysis of training checkpoints (Biderman et al., 2023) can reveal whether the $PI > RI$ asymmetry is architectural or learned. Third, *targeted mitigation*: once mechanisms are understood, principled interventions—recency-weighted attention, structured context ordering, positional debiasing (Liu et al., 2024)—become feasible.

Limitations

Our findings derive from a single experimental paradigm—the AB-AC paired-associate task. While this classic design enables controlled comparison between RI and PI, it remains unclear whether the observed patterns generalize to other interference manipulations (e.g., varied retention intervals, intervening tasks) or alternative paradigms. The dual-process interpretation, while consistent with our behavioral dissociations, requires validation through additional experimental designs.

Additional limitations include: (1) parameter counts for closed-source models are estimates; (2) synthetic category-value stimuli may not capture naturalistic interference dynamics (see Future Directions); (3) our evidence is behavioral—mechanistic validation via attention probing is discussed in Future Directions; (4) all tested models are transformer-based, excluding state-space models and base versus fine-tuned comparisons; (5) English-only testing limits cross-linguistic generalization.

Ethical Considerations

This work evaluates memory interference in LLMs through controlled experiments that do not involve human subjects or personal data. All experiments used synthetic category-value pairs specifically designed for this research. Our findings on model-specific vulnerabilities (e.g., PI susceptibility in reasoning models) aim to inform responsible deployment rather than enable misuse. We note potential dual-use concerns: understanding interference patterns could theoretically be exploited to craft adversarial prompts that confuse model memory. However, we believe the defensive value—enabling practitioners to select appropriate models

for interference-sensitive applications and anticipate failure modes—outweighs this risk. Model parameter counts for proprietary systems are estimates; we make no claims about internal architectures beyond publicly available information. We encourage replication and extension of these findings across additional languages and model families to ensure generalizability.

References

- Josh Achiam, Steven Adler, Sandhini Agarwal, Lama Ahmad, Ilge Akkaya, Florencia Leoni Aleman, Diogo Almeida, Janko Altenschmidt, Sam Altman, Shyamal Anadkat, and 1 others. 2023. Gpt-4 technical report. *arXiv preprint arXiv:2303.08774*.
- Michael C Anderson, Robert A Bjork, and Elizabeth L Bjork. 1994. Remembering can cause forgetting: Retrieval dynamics in long-term memory. *Journal of Experimental Psychology: Learning, Memory, and Cognition*, 20(5):1063–1087.
- Richard C Atkinson and Richard M Shiffrin. 1968. Human memory: A proposed system and its control processes. In *Psychology of Learning and Motivation*, volume 2, pages 89–195. Academic Press.
- Yushi Bai, Xin Lv, Jiajie Zhang, Hongchang Lyu, Jiankai Tang, Zhidian Huang, Zhengxiao Du, Xiao Liu, Aohan Zeng, Lei Hou, and 1 others. 2024. Longbench: A bilingual, multitask benchmark for long context understanding. *arXiv preprint arXiv:2308.14508*.
- Stella Biderman, Hailey Schoelkopf, Quentin Gregory Anthony, Herbie Bradley, Kyle O’Brien, Eric Hallahan, Mohammad Aflah Khan, Shivanshu Purohit, USVSN Sai Prashanth, Edward Raff, and 1 others. 2023. Pythia: A suite for analyzing large language models across training and scaling. *International Conference on Machine Learning*, pages 2397–2430.
- Tom Brown, Benjamin Mann, Nick Ryder, Melanie Subbiah, Jared D Kaplan, Prafulla Dhariwal, Arvind Neelakantan, Pranav Shyam, Girish Sastry, Amanda Askell, and 1 others. 2020. Language models are few-shot learners. *Advances in neural information processing systems*, 33:1877–1901.
- Nelson Elhage, Tristan Hume, Catherine Olsson, Nicholas Schiefer, Tom Henighan, Shauna Kravec, Zac Hatfield-Dodds, Robert Lasenby, Dawn Drain, Carol Chen, and 1 others. 2022. Toy models of superposition. *Transformer Circuits Thread*.
- Randall W Engle. 2002. Working memory capacity as executive attention. *Current directions in psychological science*, 11(1):19–23.
- Robert M French. 1999. Catastrophic forgetting in connectionist networks. *Trends in cognitive sciences*, 3(4):128–135.
- Yiwen Fu, Aaryan Gupta, Zhengxuan Jiang, Christopher Potts, and Michael S. Bernstein. 2025. Language models can’t tell what’s missing: Probing absence detection in text. *arXiv preprint arXiv:2506.11440*.
- Jordan Hoffmann, Sebastian Borgeaud, Arthur Mensch, Elena Buchatskaya, Trevor Cai, Eliza Rutherford, Diego de Las Casas, Lisa Anne Hendricks, Johannes Welbl, Aidan Clark, and 1 others. 2022. Training compute-optimal large language models. *arXiv preprint arXiv:2203.15556*.
- John G Jenkins and Karl M Dallenbach. 1924. Obliviscence during sleep and waking. *The American journal of psychology*, 35(4):605–612.
- Greg Kamradt. 2023. [Needle in a haystack - pressure testing llms](#).
- Michael J Kane and Randall W Engle. 2001. Working-memory capacity, proactive interference, and divided attention: Limits on long-term memory retrieval. *Journal of Experimental Psychology: Learning, Memory, and Cognition*, 27(2):336–358.
- Jared Kaplan, Sam McCandlish, Tom Henighan, Tom B Brown, Benjamin Chess, Rewon Child, Scott Gray, Alec Radford, Jeffrey Wu, and Dario Amodei. 2020. Scaling laws for neural language models. *arXiv preprint arXiv:2001.08361*.
- Tomáš Kočiský, Jonathan Schwarz, Phil Blunsom, Chris Dyer, Karl Moritz Hermann, Gábor Melis, and Edward Grefenstette. 2018. The NarrativeQA reading comprehension challenge. *Transactions of the Association for Computational Linguistics*, 6:317–328.
- Kunlun Ling, Yifan Weng, Shaoxiong Ji, Michalis Vazirgiannis, Zhiqiang Deng, and Min-Yen Kan. 2025. Longreason: A synthetic long-context reasoning benchmark via context expansion. *arXiv preprint arXiv:2501.15089*.
- Nelson F Liu, Kevin Lin, John Hewitt, Ashwin Paranjape, Michele Bevilacqua, Fabio Petroni, and Percy Liang. 2024. Lost in the middle: How language models use long contexts. *Transactions of the Association for Computational Linguistics*, 12:157–173.
- Colin M MacLeod. 2024. Interference theory: History and current status. In *The Oxford Handbook of Human Memory*, pages 1173–1208. Oxford University Press.
- Michael McCloskey and Neal J Cohen. 1989. Catastrophic interference in connectionist networks: The sequential learning problem. *Psychology of learning and motivation*, 24:109–165.
- Ali Modarressi, Amirhossein Deghani, Mohammad Taher Pilehvar, and Hinrich Schütze. 2025. Nollima: Long-context evaluation beyond literal matching. *Proceedings of ICML*.
- Bennet B Murdock. 1962. The serial position effect of free recall. *Journal of Experimental Psychology*, 64(5):482–488.

OpenAI. 2024. [Learning to reason with llms](#). Technical report, OpenAI.

Adam Scherlis, Kshitij Sachan, Adam S Jermyn, Joe Benton, and Buck Shlegeris. 2022. Polysemanticity and capacity in neural networks. *arXiv preprint arXiv:2210.01892*.

Benton J Underwood. 1957. Interference and forgetting. *Psychological review*, 64(1):49.

Chupeí Wang and Jiaqiu Vince Sun. 2025. Unable to forget: Proactive interference reveals working memory limits in llms beyond context length. In *ICML 2025 Workshop on Long Context Foundation Models*.

Jason Wei, Xuezhi Wang, Dale Schuurmans, Maarten Bosma, Fei Xia, Ed Chi, Quoc V Le, Denny Zhou, and 1 others. 2022. Chain-of-thought prompting elicits reasoning in large language models. *Advances in Neural Information Processing Systems*, 35:24824–24837.

Delos D Wickens. 1970. Encoding categories of words: An empirical approach to meaning. *Psychological Review*, 77(1):1–15.

John T Wixted. 2004. The psychology and neuroscience of forgetting. *Annual review of psychology*, 55:235–269.

Guangxuan Xiao, Yuandong Tian, Beidi Chen, Song Han, and Mike Lewis. 2024. Efficient streaming language models with attention sinks. In *International Conference on Learning Representations*.

A Experimental Setup

Stimuli. We used 46 semantic categories with 50–70 real-world meaningful values per category:

Arts: visual art, dance style, literary genre, painting medium. *Science:* chemical element, constellation, mathematical concept. *Nature:* bird species, flower species, tree species, weather phenomenon. *Food:* cheese variety, wine variety, pasta shape, culinary herb, fruit variety. *Culture:* ancient civilization, martial art, board game. *Technology:* programming language, telescope type, photography technique.

Example values for “fruit variety”: mangosteen, bergamot, persimmon, mirabelle, kiwi, grape, etc.

Prompt Structure. Table 4 shows the three-phase RI prompt structure.

PI Prompt: Identical structure, except the query asks “What was the *LAST* value of visual art?” Both conditions use the same stimulus sequence—only the retrieval target differs.

Phase	Content
Instruction	You will learn initial facts about categories, then see updates. Later, recall the INITIAL values you learned first.
Initial Learning	visual art: abstract expressionism tools: screwdriver ... (<i>46 categories</i>)
Updates	Following facts have been updated: visual art: baroque tools: hammer ... (<i>$N \times 46$ updates, randomized order</i>)
Query	What was the INITIAL value of visual art?

Table 4: **RI Prompt Structure.** The prompt presents initial category–value pairs, followed by N rounds of updates, then queries a single category.

Metric Definitions. Both RIES and PIES are computed as the area under the accuracy-vs-interference curve using trapezoidal integration with log-scaled x-axis. Let $\Delta_i = \log_{10}(L_{i+1} + 1) - \log_{10}(L_i + 1)$ for levels $L_i \in \{3, 10, 50, 100, 200, 300\}$:

$$\text{RIES} = \sum_{i=1}^{n-1} \frac{A_i^{\text{RI}} + A_{i+1}^{\text{RI}}}{2} \cdot \Delta_i \quad (2)$$

$$\text{PIES} = \sum_{i=1}^{n-1} \frac{A_i^{\text{PI}} + A_{i+1}^{\text{PI}}}{2} \cdot \Delta_i \quad (3)$$

where A_i^{RI} and A_i^{PI} are RI and PI accuracy at level L_i . The +1 offset accounts for the initial value presentation. Log-scaling ensures equal weighting across orders of magnitude. Higher scores indicate greater resistance.

B Model Specifications

Table 8 lists all 39 models tested with complete data across all interference levels, sorted by parameter count (descending). RIES measures resistance to retroactive interference; PIES measures resistance to proactive interference. Architecture indicates Dense or Mixture-of-Experts (MoE); Reasoning indicates chain-of-thought models. **Note:** Models with optional extended thinking (e.g., Claude-4-opus, Gemini-2.5-pro) were tested with thinking *disabled*. Only models that use chain-of-thought by default (o-series, DeepSeek-R1) are classified as reasoning.

Models are grouped into four size tiers (Table 5) for decay curve analysis. The testbed spans seven model families (OpenAI, Anthropic, Google, Meta,

Amazon, Alibaba, DeepSeek) covering parameter counts from 1B to 2,500B, both Dense and MoE architectures, and both standard and reasoning configurations.

Tier	Parameters	n	Examples
XS	$\leq 10\text{B}$	5	Llama-3.2-1b, Nova-micro
S	11–99B	10	Llama-3.2-90b, o4-mini
M	100–670B	13	Claude-4.5-opus, Llama-3.1-405b
L	$\geq 671\text{B}$	11	GPT-5, o1, DeepSeek-R1

Table 5: **Size Tier Definitions.** Parameter-based grouping used for decay curve analysis (Figures 5–6).

C Error Type Taxonomy

All incorrect responses (5,409 total across 39 models and 6 interference levels) were classified into five mutually exclusive error types (Table 6). Examples assume the query asks for the *initial* value of “visual art” (correct: “abstract expressionism”), with N updates reassigning it to “baroque,” “cubism,” etc. Table 7 shows how the distribution shifts across interference levels.

Error Type	%	Definition & Example
Same-Key Interf.	46.0	Value from correct category, wrong position. “ <i>baroque</i> ”
Retrieval Failure	50.8	No value produced; refusal or empty. “ <i>I’m not sure</i> ”
Partial Match	1.8	Truncated or recombined. “ <i>abstract express</i> ”
Hallucination	0.9	Plausible but never presented. “ <i>impressionism</i> ”
Cross-Key Interf.	0.6	Value from a different category. “ <i>screwdriver</i> ”

Table 6: **Error Type Taxonomy.** Five mutually exclusive error categories ($n=5,409$ total errors). Sorted by frequency.

Error Type	Low $N=3,10$	Moderate $N=50,100$	High $N=200,300$
Same-Key Interf.	6.4%	25.8%	55.8%
Cross-Key Interf.	1.8%	0.3%	0.5%
Hallucination	4.5%	1.1%	0.1%
Retrieval Failure	80.1%	72.9%	42.0%

Table 7: **Error Distribution by Interference Stage.** At low interference, errors are dominated by retrieval failures. As interference increases, same-key intrusions progressively dominate, indicating that competing memories become strong enough to override the target rather than simply blocking retrieval.

D Detailed Results by Model and Condition

D.1 Top and Bottom Performers

Table 9 shows RI and PI accuracy at each interference level for the five highest- and lowest-scoring models. RI top performers are reasoning models maintaining near-ceiling accuracy; PI top performers are exclusively Claude models. Notably, o1 ranks #1 for RI but appears in the PI bottom 5 at 0%—the starkest dual-process dissociation.

D.2 Reasoning vs Non-Reasoning Models

The six reasoning models (o1, o1-preview, o3, o3-mini, o4-mini, DeepSeek-R1) exhibit the most extreme RI–PI dissociation. Table 10 compares mean accuracy by interference level; Table 11 provides the per-model breakdown.

Why 0% PI accuracy? The 0% scores do *not* reflect refusals or empty responses. These models respond confidently with all 46 category values—but consistently return values from *earlier* positions rather than the most recent ones. The chain-of-thought process appears to consolidate earlier encodings so strongly that recent updates become inaccessible, even when the prompt explicitly requests the “LAST value.” This is primacy intrusion, not retrieval failure. Table 12 shows a representative example.

E Additional Figures

This section presents supplementary visualizations that complement the tabular results above. Figures 5–6 show RI and PI decay curves stratified by model size tier. Figure 7 contrasts reasoning and non-reasoning models. Figures 8–9 provide detailed error pattern visualizations.

Model	B	Arch	Rea.	RIES	PIES	Model	B	Arch	Rea.	RIES	PIES
GPT-5	2500	MoE	N	186.4	99.2	Gemini-2.0-flash	100	MoE	N	162.5	101.6
GPT-5-mini	2500	MoE	N	162.5	109.1	Gemini-2.0-flash-lite	100	MoE	N	143.9	98.6
GPT-5-nano	2500	MoE	N	160.6	21.0	Llama-3.2-90b	90	Dense	N	134.6	87.1
o3	2000	MoE	Y	185.8	76.0	Nova-pro	70	Dense	N	157.5	63.7
o3-mini	2000	MoE	Y	183.3	75.6	Llama-3.1-70b	70	Dense	N	134.6	87.1
o1	1760	MoE	Y	186.4	22.0	Llama-3.3-70b	70	Dense	N	138.7	100.3
o1-preview	1760	MoE	Y	186.4	76.0	Gemini-2.5-flash-lite	40	MoE	N	146.3	91.3
GPT-4.1	1760	MoE	N	176.9	118.6	o4-mini	30	MoE	Y	170.5	22.0
GPT-4.1-mini	1760	MoE	N	157.6	116.9	Qwen-3-coder-30b	30	MoE	N	166.4	89.3
GPT-4.1-nano	1760	MoE	N	128.2	73.9	Claude-4.5-haiku	15	Dense	N	142.6	128.5
DeepSeek-R1	671	Dense	Y	155.4	55.6	Llama-3.2-11b	11	Dense	N	138.4	47.6
Llama-3.1-405b	405	Dense	N	141.7	57.2	Claude-3.5-haiku	10	Dense	N	139.8	126.4
Llama-4-maverick	400	MoE	N	178.3	67.9	Llama-3.1-8b	8	Dense	N	128.3	57.1
Claude-4.5-opus	300	Dense	N	178.4	170.3	Nova-lite	7	Dense	N	130.7	53.2
Gemini-2.5-pro	300	MoE	N	162.5	123.6	Llama-3.2-3b	3	Dense	N	113.6	16.8
Claude-4.5-sonnet	250	Dense	N	162.5	124.2	Nova-micro	1	Dense	N	126.1	76.8
Qwen-3-VL-235b	235	MoE	N	177.3	120.2	Llama-3.2-1b	1	Dense	N	126.1	1.0
Claude-4-opus	200	Dense	N	139.6	131.0						
Claude-4-sonnet	200	Dense	N	162.5	137.8						
Claude-3-opus	175	Dense	N	145.2	131.5						
GPT-3.5-turbo	175	MoE	N	156.1	120.0						
Llama-4-scout	109	MoE	N	153.9	40.2						

B = parameters in billions
Rea. = reasoning model (Y/N)

Table 8: **Complete Model Specifications.** All 39 models with RIES and PIES scores. Models sorted by parameter count (descending). See Section B for details.

Model	RI Accuracy (%)						Model	PI Accuracy (%)					
	3	10	50	100	200	300		3	10	50	100	200	300
<i>Top 5 (highest RIES)</i>							<i>Top 5 (highest PIES)</i>						
o1	100	97.8	98.6	100	100	100	Claude-4.5-opus	100	97.8	91.3	80.4	84.8	71.7
o1-preview	100	97.8	100	100	98.6	99.3	Claude-4-sonnet	100	97.8	93.5	34.8	23.9	8.7
GPT-5	100	97.8	100	100	98.6	38.4	Claude-3-opus	100	84.8	95.7	32.6	28.3	2.2
o3	100	97.8	100	99.3	99.3	100	Claude-4-opus	100	91.3	91.3	30.4	21.7	4.3
o3-mini	100	97.8	100	65.9	43.5	68.1	Claude-4.5-haiku	100	93.5	95.7	19.6	10.9	4.3
<i>Bottom 5 (lowest RIES)</i>							<i>Bottom 5 (lowest PIES)</i>						
Llama-3.1-8b	58.7	97.8	89.1	43.5	16.7	13.8	o1	100	0	0	0	0	0
GPT-4.1-nano	82.6	71.0	87.7	56.5	23.9	6.5	o4-mini	100	0	0	0	0	0
Nova-micro	94.9	89.1	69.6	35.5	15.2	2.2	GPT-5-nano	95.7	0	0	0	0	0
Llama-3.2-1b	73.9	97.8	81.9	56.5	0	2.2	Llama-3.2-3b	73.9	0	0	0	2.2	0
Llama-3.2-3b	0	89.1	97.8	21.7	17.4	76.1	Llama-3.2-1b	2.2	0	0	0	2.2	0

Table 9: **RI and PI Accuracy (%) at Each Interference Level.** Top 5 and bottom 5 models by RIES (left) and PIES (right).

	3	10	50	100	200	300
<i>RI Accuracy (%)</i>						
Reasoning	100	97.8	99.8	94.1	82.0	73.4
Non-reasoning	92.8	92.9	95.3	69.1	38.9	15.7
Δ	+7.2	+4.9	+4.4	+25.0	+43.1	+57.7
<i>PI Accuracy (%)</i>						
Reasoning	99.6	59.1	0	0	0	0
Non-reasoning	93.5	69.4	53.6	10.9	9.9	3.4
Δ	+6.2	-10.3	-53.6	-10.9	-9.9	-3.4

Table 10: **Reasoning vs Non-Reasoning Models.** Mean accuracy by interference level. Reasoning models show a widening RI advantage (+57.7% at $N=300$) but catastrophic PI failure (0% from $N=50$ onward).

Model	RI Accuracy (%)						PI Accuracy (%)					
	3	10	50	100	200	300	3	10	50	100	200	300
o1	100	97.8	98.6	100	100	100	100	0	0	0	0	0
o1-preview	100	97.8	100	100	98.6	99.3	100	97.8	0	0	0	0
o3	100	97.8	100	99.3	99.3	100	100	97.8	0	0	0	0
o3-mini	100	97.8	100	65.9	43.5	68.1	97.8	97.8	0	0	0	0
o4-mini	100	97.8	100	100	55.1	5.8	100	0	0	0	0	0
DeepSeek-R1	100	97.8	100	99.3	95.7	67.4	100	60.9	0	0	0	0

Table 11: **Reasoning Models: RI vs PI Accuracy at Each Interference Level.** Most models maintain high RI accuracy through $N=100$, though o3-mini and o4-mini degrade earlier. All six collapse to 0% PI by $N=50$, with o1 and o4-mini failing at $N=10$ —the earliest collapse point.

Field	Value
Model	o1
Condition	PI, $N=300$
Category	visual art
Expected (last)	land art (update #300)
Returned	“neo pop 176” (update #176)

The model responds confidently with position-indexed values: “visual art → neo pop 176”—returning update #176 out of 300, not the last. Despite explicitly tracking updates (“I have carefully tracked every update...”), it retrieves mid-sequence values. Accuracy: 0/46 (0%). The model’s reasoning process cannot overcome primacy bias.

Table 12: **Example PI Failure: o1 at $N=300$.** The model returns earlier update values (with position indices) instead of the most recent ones, demonstrating primacy intrusion despite explicit chain-of-thought reasoning.

Field	Value
Model	Claude-4.5-haiku
Condition	RI, $N=300$
Category	literary genre
Expected (initial)	memoir
Returned	hard sci fi

The model returns “hard sci fi” (a later update value) instead of the initial value “memoir.” At $N=300$, with 300 intervening updates per category, the initial encoding has been overwritten by subsequent information. Accuracy: 4/46 (8.7%). Unlike PI failures where earlier values intrude, RI failures show later values displacing the original—recency overwrites primacy.

Table 13: **Example RI Failure: Claude-4.5-haiku at $N=300$.** The model returns a later update value instead of the initial one, demonstrating how retroactive interference overwrites early encodings with recent information.

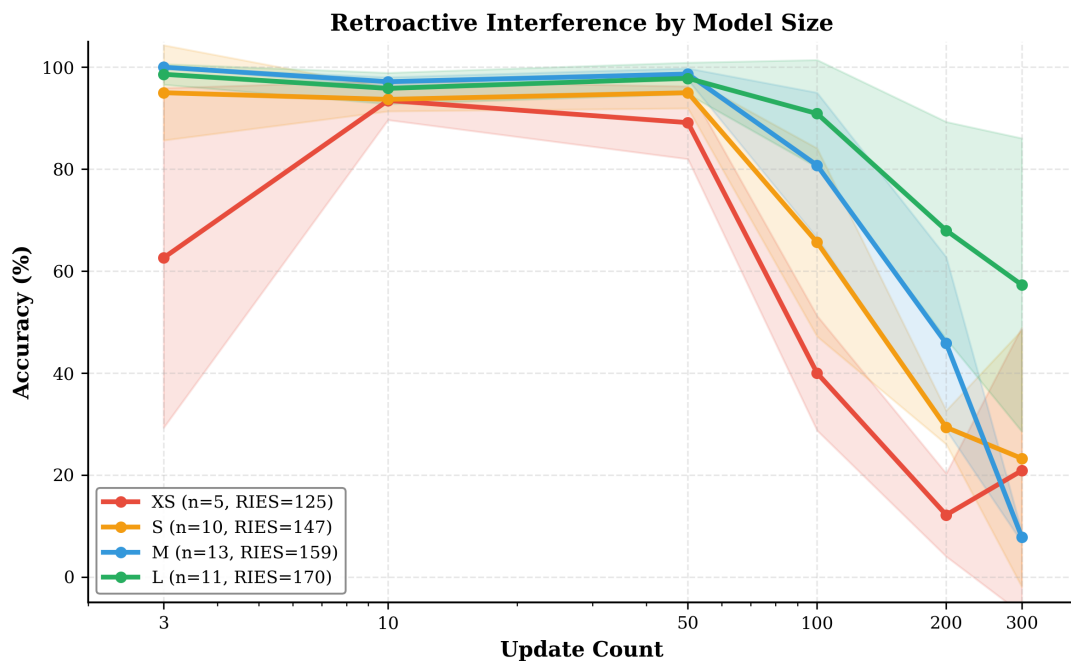


Figure 5: **RI Decay Curves by Model Size Tier.** Larger models (>100B parameters) maintain higher accuracy across all interference levels. The decay pattern shows that size provides consistent protection against retroactive interference, with the largest models maintaining >50% accuracy even at N=300.

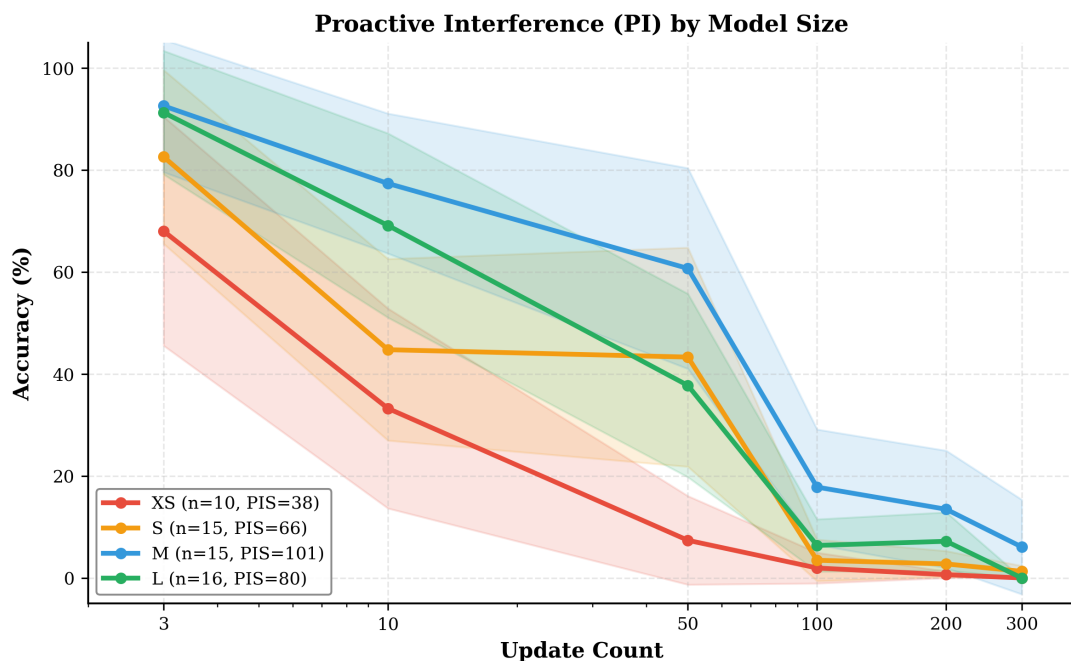


Figure 6: **PI Decay Curves by Model Size Tier.** Unlike RI (Figure 5), PI decay shows no consistent relationship with model size ($R^2 = 0.06$, n.s.). Medium-sized models (M tier, blue) actually outperform large models (L tier, green) at high interference levels. This lack of size-dependence, contrasting with RI's strong size correlation ($R^2 = 0.49$), provides evidence that PI is architecture-constrained rather than capacity-limited.

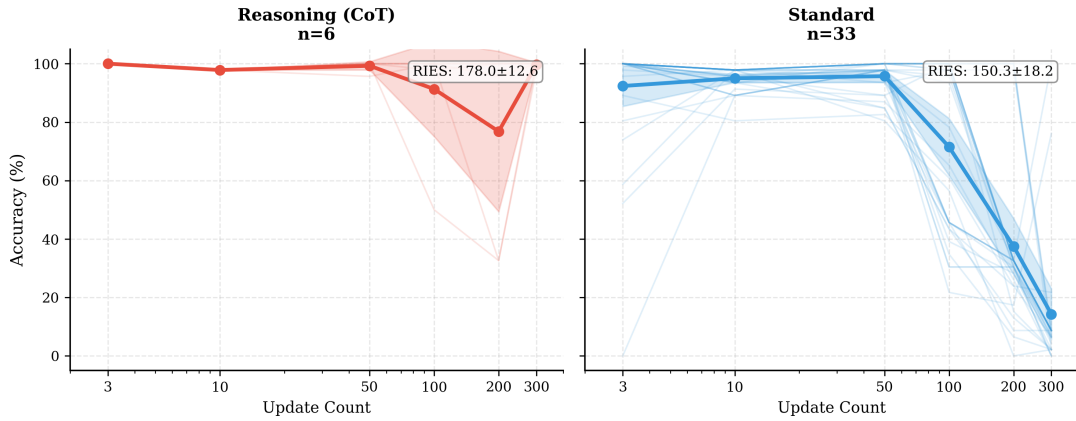


Figure 7: **RI Decay Curves: Reasoning vs Non-Reasoning Models.** Chain-of-thought reasoning models (solid lines) show markedly slower decay compared to standard models (dashed lines). Extended inference-time computation appears to enhance memory consolidation, with reasoning models maintaining higher accuracy at all interference levels.

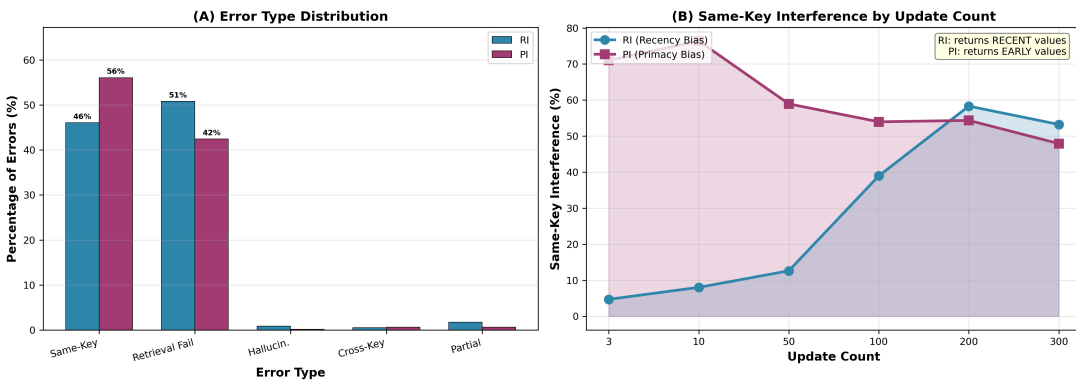


Figure 8: **Detailed Error Pattern Analysis.** Distribution of error types across RI and PI conditions. RI errors are predominantly retrieval failures (50.8%), while PI errors show primacy intrusion (56.1% same-key interference). Both conditions show minimal hallucination (<1%), confirming that models confuse positions rather than fabricate values.

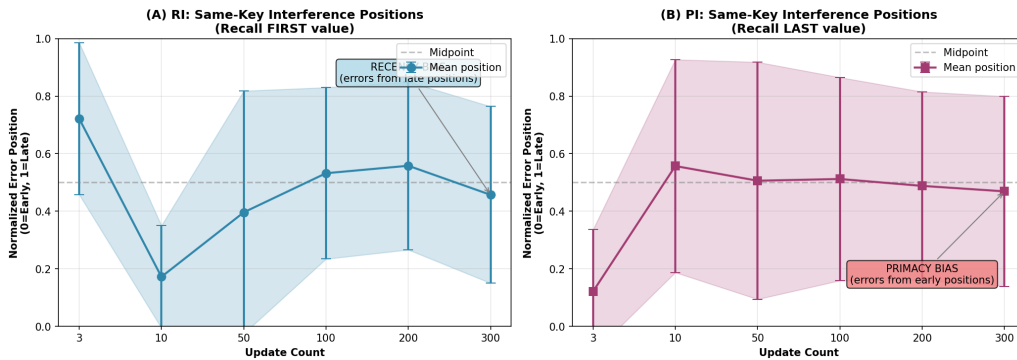


Figure 9: **Position-Based Error Analysis.** When same-key intrusions occur, RI errors come from middle-to-late positions (recency bias), while PI errors come from early positions with 14% returning the first value (primacy bias). This opposing directionality provides mechanistic evidence for distinct retrieval dynamics.

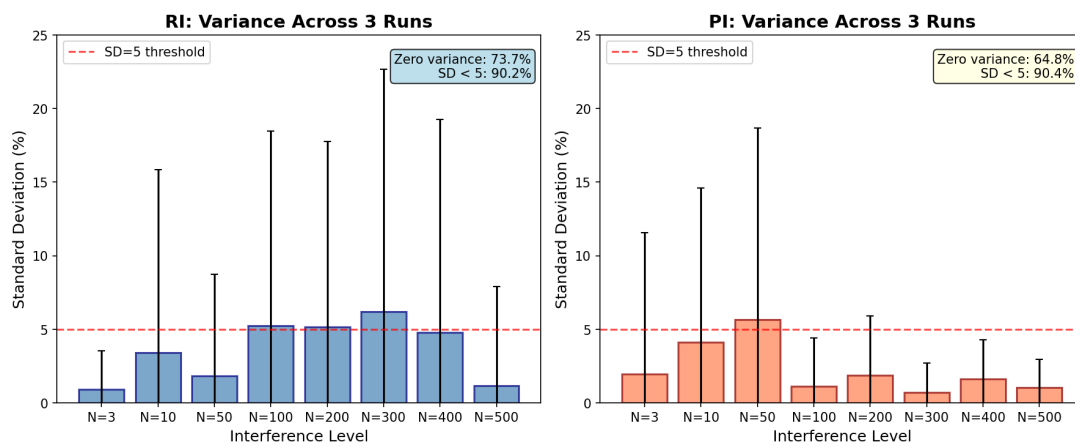


Figure 10: **Run-to-Run Variance Distribution.** Standard deviation of accuracy across 3 independent runs, aggregated by interference level for RI (blue) and PI (orange). Both conditions show high reproducibility: the majority of model-level measurements exhibit zero or near-zero variance (RI: 73.7% exact zero, 90.2% SD < 5; PI: 64.8% exact zero, 90.4% SD < 5). Comparable variance distributions confirm that the asymmetric RI vs. PI findings reflect genuine model behavior rather than measurement noise.